

Solid-State NMR on Bacterial Cells: Selective Cell Wall Signal Enhancement and Resolution Improvement using Dynamic Nuclear Polarization

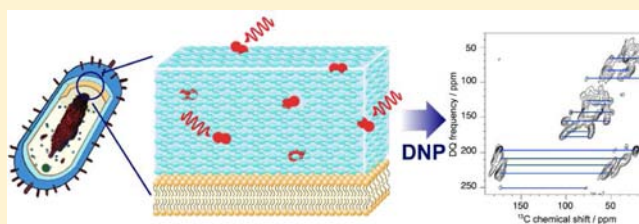
Hiroki Takahashi,[†] Isabel Ayala,[‡] Michel Bardet,[†] Gaël De Paëpe,[†] Jean-Pierre Simorre,[‡] and Sabine Hediger^{*†}

[†]Laboratoire de Chimie Inorganique et Biologique, UMR-E3 (CEA/UJF) and CNRS, Institut Nanosciences et Cryogénie, CEA, 38054 Grenoble, France

[‡]Institut de Biologie Structurale, UMR5075 (CEA/CNRS/UJF), 38027 Grenoble, France

Supporting Information

ABSTRACT: Dynamic nuclear polarization (DNP) enhanced solid-state nuclear magnetic resonance (NMR) has recently emerged as a powerful technique for the study of material surfaces. In this study, we demonstrate its potential to investigate cell surface in intact cells. Using *Bacillus subtilis* bacterial cells as an example, it is shown that the polarizing agent 1-(TEMPO-4-oxy)-3-(TEMPO-4-amino)propan-2-ol (TOTAPOL) has a strong binding affinity to cell wall polymers (peptidoglycan). This particular interaction is thoroughly investigated with a systematic study on extracted cell wall materials, disrupted cells, and entire cells, which proved that TOTAPOL is mainly accumulating in the cell wall. This property is used on one hand to selectively enhance or suppress cell wall signals by controlling radical concentrations and on the other hand to improve spectral resolution by means of a difference spectrum. Comparing DNP-enhanced and conventional solid-state NMR, an absolute sensitivity ratio of 24 was obtained on the entire cell sample. This important increase in sensitivity together with the possibility of enhancing specifically cell wall signals and improving resolution really opens new avenues for the use of DNP-enhanced solid-state NMR as an on-cell investigation tool.



INTRODUCTION

In microbiology, many molecular mechanisms, such as host-pathogen recognition, cell adhesion, or regulation of cell activity, involve interactions with the cell surface. Structural characterization of cell surface is thus of crucial importance to understand the cell life and interaction with its environment. In addition to phospholipid membranes, most biological cells have a shell of glycoconjugates at their surface, which plays a crucial role in all recognition processes. They build a complex polymorphic network around the cell and are as such difficult to characterize by classical techniques. Solid-state nuclear magnetic resonance (SSNMR) has proven to be useful for their structural study, with examples on extracted plant and bacterial cell walls.^{1–5} However, the inherent low sensitivity of NMR still often remains a limitation to answer relevant biochemical questions, especially in cases where the entire cell has to be taken into account.

Among the different existing hyperpolarizing techniques, high-field dynamic nuclear polarization (DNP) has recently emerged as a viable technique to significantly enhance the sensitivity of high-resolution SSNMR.^{6–9} In particular, it has been proven to be useful for the study of catalytic surface material.^{10,11} Similarly, DNP-enhanced SSNMR may be an interesting technique to investigate the structure of cell interface. The feasibility of applying SSNMR and more

specifically DNP-enhanced SSNMR to cell extracts or entire cells has been demonstrated recently in the context of overexpressed membrane proteins and their study.^{12,13} Using here the bacterial cell as a model, we investigate the pertinence of using DNP-enhanced SSNMR for the specific study of cell surface or cell envelope in entire cells. The bacterial cell wall is composed mainly of peptidoglycan¹⁴ which surrounds the cytoplasmic membrane and has a direct impact on the virulence and adherence of the bacteria. It plays a key role as a target of the immune response and of antibacterial treatment.^{15,16} Besides its own interest, the bacterial cell serves here as a model system to illustrate the potential of DNP-enhanced SSNMR for on-cell applications. For this purpose, essential aspects, such as optimal sample preparation, distribution of polarizing agent in the sample, and line broadening, will be here considered. We will show that under certain conditions, the sensitivity enhancement of DNP can be specifically applied to the cell surface, opening a new investigation tool for on-cell studies.

For DNP experiments typically performed at ~100 K, samples are usually suspended in a DNP matrix containing solvents, a cryoprotectant, such as *d*₈-glycerol or *d*₆-dimethyl

Received: December 21, 2012

Published: January 30, 2013

sulfoxide (DMSO), and the polarizing agent. For biological applications, the biradical TOTAPOL¹⁷ is mainly used at a concentration of 5–60 mM.^{12,13,18–21} It has to be adjusted to obtain a compromise between the optimal DNP sensitivity enhancement and the degradation of the spectrum sensitivity through line broadening, signal bleaching, and signal decays ($T_{1\rho}$ and T_2' decays) caused by paramagnetic effects.^{21–23} In addition, potential specific interaction of the radical molecule with parts of the sample, e.g., surface of proteins, lipids, cells, etc., has to be taken into account, as it would lead to a nonuniform distribution of active radicals inside the sample.

Since DNP experiments are performed at low temperature, line broadening caused by conformational disorder becomes a serious problem,^{24,25} in particular for biological samples, such as cells which may present a high degree of dynamics at room temperature. This line broadening can be important enough to cancel the gain acquired by DNP.²³ Use of crystalline solids prevents line broadening^{18,23,26} but is not feasible in the case of intact cell systems.

In this study, we clearly demonstrate for the first time the binding property of TOTAPOL to bacterial cell wall polymers in extracted sacculi as well as in entire cells. This property may be very useful to observe different compartments of the cell by either enlightening signals from the cell wall or saturating them in order to better access signals from other cell components, as required, e.g., for in-cell NMR.^{12,27} In addition, resolution enhancement of the spectra can be obtained by combining contributions obtained at low and high polarizing-agent concentrations (here TOTAPOL).

EXPERIMENTAL SECTION

Sample Preparation. Interaction of TOTAPOL with the cell wall polymers has been investigated on ¹³C-labeled *Bacillus subtilis* entire cells (EC) as well as on disrupted cells (DC) and extracted cell wall material (CWM). Gram-positive *B. subtilis* subsp. *subtilis* strain 168 cells were grown in standard ¹³C-, ¹⁵N-labeled M9 minimum medium. Cells were harvested by centrifugation at an optical density (OD, 600 nm) of about 0.7. EC were stored at 253 K in presence of 30% DMSO as cryoprotectant. DMSO is used at 10% in biology to cryopreserve more fragile eukaryotic cells.^{28,29} As a control of the resistance of *B. subtilis* cells to the DNP conditions, cell cultures were able to restart in LB medium and on agar plates by incubating, at 37 °C, cells originating from the NMR rotor after DNP experiments. Highly purified CWM were obtained by a previously published procedure after boiling the entire cells in 4% SDS (sodium dodecyl sulfate).^{30,31} This procedure retained the intact cell envelope (sacculi) formed by the peptidoglycan (PG) and covalently linked wall teichoic acids (WTAs). DC were obtained by resuspension of EC in M9 medium in presence of beads (FastPrep24). This solution was agitated at 4 °C during 20 s at a speed of 5 m/s.

For DNP experiments, fresh EC, DC, and CWM samples were first resuspended with a DNP matrix composed of *d*₆-DMSO/D₂O/H₂O in a volume ratio of 30:60:10 with various concentrations of TOTAPOL and then centrifuged back (12 000 g) to recover the pellet. For each washing step, the volume of DNP matrix used was five times larger than the cell or CWM pellet. Note that a resuspension time of ~1 min in the DNP matrix is long enough to equilibrate the TOTAPOL concentration in the sample (see Supporting Information (SI), Section 2). The samples were finally centrifuged directly into a 3.2 mm sapphire rotor closed with a silicone soft plug and a zirconia cap. In all steps, care has been taken to avoid cell degradation by cooling down samples in ice whenever possible.

DNP-Enhanced SSNMR Experiments. All spectra were recorded on a Bruker AVANCE III 400 MHz spectrometer equipped with a 263 GHz gyrotron, a transmission line, and a low-temperature 3.2 mm magic angle spinning (MAS) probe.⁹ NMR experiments were

performed at a sample temperature of 105 K and at MAS frequencies of 8.5 and 13 kHz for one- (1D) and two-dimensional (2D) experiments, respectively, unless otherwise stated. DNP enhancement factors (ϵ_{DNP}) were measured by comparing spectral intensity on the same samples at identical conditions with and without microwave (μw) irradiations. Other experimental conditions are described in the SI Section 1.

RESULTS AND DISCUSSION

Binding Affinity of TOTAPOL to PG. Figure 1 displays the effect of the successive washing steps on the DNP spectrum of

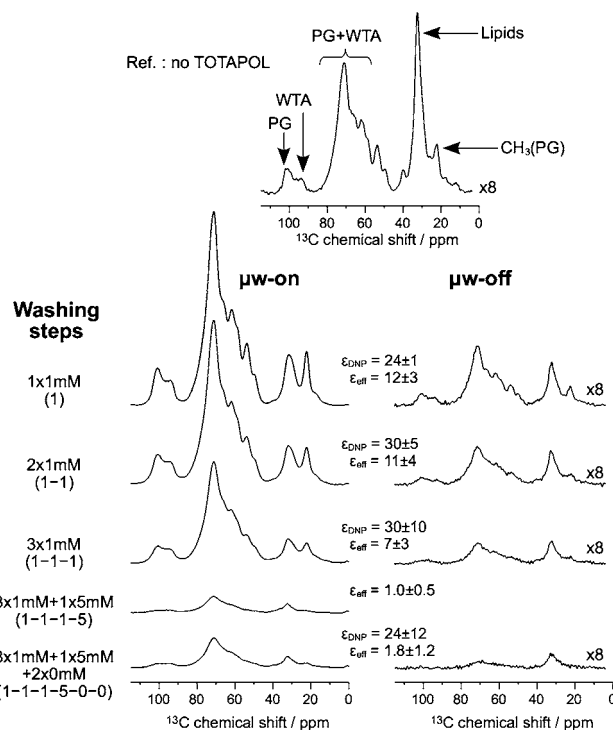


Figure 1. 1D ¹³C-CPMAS spectra on CWM recorded at various TOTAPOL concentrations with and without (left and right columns, respectively) μw irradiations. Washing steps are explained in the text and indicated. The range of ϵ_{DNP} and of effective DNP gains ϵ_{eff} found on average for the CWM signals are given. Errors reflect the heterogeneity of ϵ_{DNP} or ϵ_{eff} over the different peaks of the spectra. For the reference spectrum on the top of the figure, CWM sacculi were washed twice with the DNP matrix containing no TOTAPOL. For all spectra, a recycle delay of 25 s was used, corresponding to 1.3 times the longest measured recovery time in the reference spectrum.

CWM. Between each washing step, DNP-enhanced cross-polarization spectra under MAS (CPMAS) with and without μw irradiations have been acquired and are compared to a reference spectrum taken at the same experimental conditions but on a sample containing no TOTAPOL. The first three washing steps were performed with an identical TOTAPOL concentration of 1 mM which is much lower than what has typically been reported for similar biomolecular systems.^{12,13} Large ϵ_{DNP} of 20–40 is obtained, which remains almost constant from the first (1) to the third washing steps (1–1–1). However, a clear drop of the absolute intensity of the DNP spectra is observed with increasing number of washing steps. This drop is quantified by ϵ_{eff} which compares the μw on spectrum with the reference spectrum without TOTAPOL and which therefore includes signal bleaching caused by paramagnetic effects.

In addition to the decrease of the signal intensities, a clear broadening of the linewidths appears, and the DNP build-up time constant (τ_{DNP}) measured by a saturation-recovery experiment is shortened from 2.6 s on average after the first washing step to 0.8 s after the third one (see Figure 2). τ_{DNP}

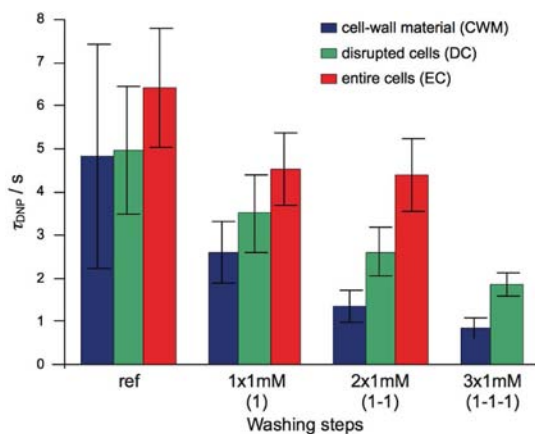


Figure 2. DNP build-up time constant τ_{DNP} averaged over the different cell wall peaks of the 1D spectra on CWM (blue), DC (green), and EC (red) samples, recorded at different TOTAPOL concentrations. Error bars reflect the heterogeneity of τ_{DNP} over the different peaks of the spectra. Measurement of EC at (1–1–1) washing step has not been measured, but values at higher TOTAPOL concentrations are given in Figure S3.

corresponds to the longitudinal relaxation time constant T_1 in standard NMR experiments (without DNP). When the DNP mechanism relies on cross effect,^{32–34} which is the case here, τ_{DNP} is usually very close to T_1 .^{35–37} The decrease in the value of τ_{DNP} is a clear indication of an enhanced relaxation mechanism. As all experimental parameters impacting the relaxation are kept constant, a change in the radical concentration in the sample has to be considered. Taking into account the reduction in τ_{DNP} and the resulting possibility to shorten the delay between successive acquisitions, the sample washed three times with 1 mM TOTAPOL (1–1–1) proves to have the optimum effective DNP enhancement ‘per unit time’, with a slightly degraded resolution. In the case of more advanced pulse sequences, signal decays during mixing periods should also be considered to determine optimal enhancements, since $T_{1\rho}$ and T_2' decays also largely depend on the concentration of polarizing agents.

When the CWM sample is further resuspended with the DNP matrix containing 5 mM TOTAPOL (1–1–1–5), a significant line broadening is observed, and the DNP signal intensity collapses strongly due to further signal bleaching. In fact, with ϵ_{eff} between 0.4–1.5, no effective sensitivity enhancement by DNP is obtained. τ_{DNP} is reduced to 0.3 s on average. Interestingly, this trend in the spectral features could not be reversed by rinsing the sample twice with DNP matrix containing no TOTAPOL (1–1–1–5–0–0). Since the volume of the DNP matrix (without TOTAPOL) used for rinsing is five times larger than that of the CWM pellet, which is supposed to contain 5 mM TOTAPOL, the concentration of TOTAPOL after washing is expected to be reduced to 0.14 mM, provided a particular affinity does not exist. However, major signal bleaching ($\epsilon_{\text{eff}} = 0.5 - 3$), short DNP build-up ($\tau_{\text{DNP}} = 0.4$ s, Figure S3), and strong line broadening are still observed. These findings all suggest that the TOTAPOL

molecules accumulate into the CWM polymer network along with the successive washing steps, even when the concentration of the matrix used for washing is kept constant. As stated in the Experimental Section, the resuspending time in the DNP matrix is long enough for TOTAPOL to equilibrate (see also SI Section 2). These observations can therefore only be explained by the presence of a strong binding affinity of TOTAPOL to CWM polymers.

A similar affinity has been recently postulated in the case of cellulose, to explain the very high DNP absolute sensitivity ratio (ASR) obtained on a matrix-free sample.²³ As both PG and cellulose contain sugar chains, we suggest that TOTAPOL molecules interact with sugars, probably via hydrogen bonding. This is further confirmed by comparing the DNP signal enhancement on sugars (60–80 ppm) and residual lipids (~33 ppm), being 25 and 8, respectively, in the one-time 1 mM washed sample (Figure 1, washing step 1). This indicates that the TOTAPOL concentration is higher in the cell wall itself than in the surrounding solution. The unlabeled DMSO signal (~38 ppm) is buried under the lipid signal. Its enhancement factor is expected to be similar to that of lipids.

Affinity of TOTAPOL in Entire Cells and Disrupted Cells.

The affinity of TOTAPOL to PG explains why such a large DNP enhancement is obtained on the CWM sample prepared with DNP matrix at a very low TOTAPOL concentration (1 mM). Indeed, TOTAPOL molecules are trapped in the CWM, and the effective final concentration in the cell wall is therefore higher than originally in the matrix. This feature may be very useful to specifically enhance signals of the cell wall in order to study its structure or interactions in entire cells.

To evaluate the pertinence of this strategy, a similar series of experiments with sequential washing steps have been performed on *B. Subtilis* entire cells (EC sample) (Figure S4). The optimum sensitivity per unit time found for EC is one-wash with 5 mM TOTAPOL solution ($\epsilon_{\text{DNP}} = 16-18$ and $\epsilon_{\text{eff}} = 7-11$). A similar behavior indicating accumulation of TOTAPOL is observed on entire cells as it was for CWM but at higher TOTAPOL concentrations. This behavior is also observed on the DNP build-up time constant τ_{DNP} as seen in Figures 2 and S3. This shift to higher concentrations can be explained by a lower accessibility of TOTAPOL to the PG due to the presence of surface proteins and the incapacity for TOTAPOL to enter the cells.

DC possesses an intermediate accessibility to the PG, as the cell walls are now broken, but the surface and membrane proteins are still present within PG. The spectral behavior along the different washing steps (Figure S5) and τ_{DNP} (Figures 2 and S3) show again the same accumulation of TOTAPOL in the sample but at intermediate concentrations between CWM and EC. In the presence of purified sacculi (CWM), TOTAPOL molecules can access everywhere on the PG, while they can only access from the outer cell surface with EC. With DC, they can travel through the cell membrane but accessibility to PG is still limited by the presence of membrane proteins, lipids, etc.

Considering that radical molecules are mainly trapped inside the cell wall and that a gradient in TOTAPOL concentration is probably present with higher concentrations at the outer surface, the question of the distance covered by DNP-enhanced polarization comes up. Estimation of this distance is difficult and complex, as it relies on the proton spin-diffusion rate D which is not readily available. A pseudo-1D model of polarization transfer depth has been developed for the case of

amyloid crystals.¹⁸ With this model and their estimation of D , a distance of several hundreds of nm can be covered. The system considered here is however very different from an amyloid crystal, and several aspects, such as residual mobility, deuteration of the DNP matrix,³⁸ and the consequently dilution of protons,³⁹ are expected to decrease strongly the spin-diffusion rate (see SI Section 5). A reduction of D by a factor of 20 leads to a polarization transfer depth (at half of the original intensity) of 30–50 nm, which is on the order of magnitude of the cell wall thickness in *B. subtilis*.

Absolute Sensitivity Ratio (ASR). It is worth noting that the parameter ϵ_{DNP} , usually evaluated for DNP experiments, did not change significantly with the successive washing steps and therefore did not reflect the pertinence of the DNP experiment. For a real estimation of the sensitivity enhancement obtained by DNP, it is important to always consider ϵ_{eff} that is obtained by comparing a μW -on spectrum to a reference (no TOTAPOL) spectrum. This comparison therefore includes signal bleaching due to the presence of polarizing agents. More generally, the ASR,²³ which is the real sensitivity gain obtained by comparing the signal-to-noise (S/N) per unit time on the DNP experiment and on the conventional NMR experiment, needs to be evaluated to discuss the usefulness of DNP.

Figure 3 compares 1D ^{13}C -CPMAS spectra of EC obtained by DNP-enhanced SSNMR and conventional NMR. Note that

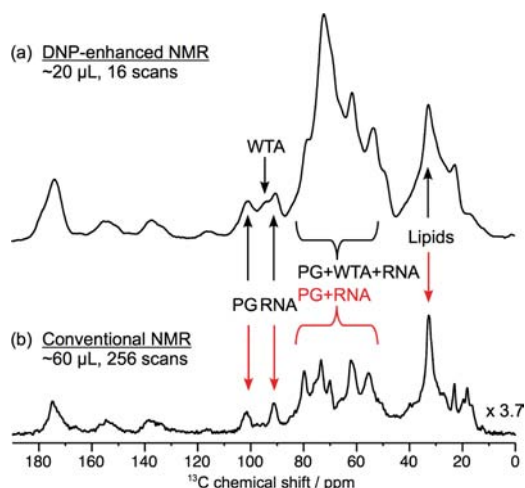


Figure 3. Comparison of 1D ^{13}C -CPMAS spectra of EC obtained using DNP-enhanced NMR at 105 K (a) and conventional NMR at ~ 270 K (b). Recycle delays are 4 s for the DNP experiment and 1 s for the conventional NMR. Both spectra were recorded at 9.4 T (^1H : 400 MHz) and 13 kHz MAS frequency, using a 3.2 and 4 mm rotor for the DNP and conventional NMR experiments, respectively. The 4 mm rotor contains about three times more sample than the 3.2 mm one. Spectra (a) and (b) were obtained with 16 and 256 transients, respectively.

the bacterial cell pellet used was three times larger for the conventional NMR than for the DNP-enhanced NMR sample. In these conditions, ASRs were 15, 24, and 9 on carbonyl, sugars, and lipid resonances, respectively, which lead to a time savings of up to a factor of 600. This order of magnitude in absolute sensitivity enhancement really opens new avenues in the study of cell walls, e.g., the detection of a small number of molecules being able to interact with the cell wall, which cannot be detected by conventional NMR even on ^{13}C -labeled systems. In fact, we recently demonstrated that a similar

value of ASR allowed the acquisition of natural abundance 2D ^{13}C – ^{13}C correlation experiments in tens of minutes of experimental time using DNP,²³ even though cross-peak intensities are 4 orders of magnitude smaller than in ^{13}C -labeled systems. The study of cell wall interactions should therefore also be feasible using cell wall-enhanced DNP technique as described here.

Stability of EC during Long-Time Storage. As deterioration of TOTAPOL radicals have been reported on the membrane protein neurotoxin II after long-time storage (4–8 weeks),⁴⁰ the stability of the EC sample was also investigated. After 6 months in the freezer at 253 K, no change in the 1D CPMAS and 2D ^{13}C – ^{13}C DARR (dipolar assisted rotational resonance) spectra were observed (Figure S7). ϵ_{DNP} and the linewidths are almost unchanged indicating that all TOTAPOL radicals are still active. Similarly, no deterioration of the radical was reported for SH3⁴¹ that does not possess any cysteine residues that are thought to react with TOTAPOL radicals.

Cell Wall Enhancement and Suppression. According to the above discussion, we can conclude that TOTAPOL molecules are preferably located in the PG layer of the bacterial cell envelope. At low concentrations of radical, signals belonging to the cell wall are particularly enhanced by DNP compared to signals from the rest of the cell. Quite the opposite, we expect that high concentrations of TOTAPOL will bleach the cell wall signals and highlight signals from other distinct cell components, e.g., RNA and lipids. This is indeed observed in 1D DNP-enhanced ^{13}C -CPMAS spectra acquired on EC at various TOTAPOL concentrations (Figure 4). With

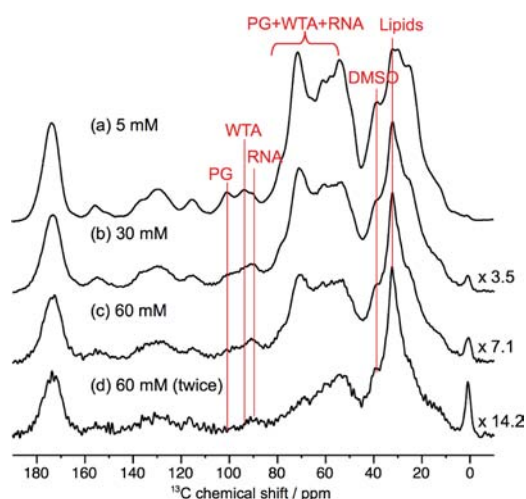


Figure 4. 1D DNP-enhanced ^{13}C -CPMAS spectra on EC at various TOTAPOL concentrations recorded with 16 transients at 105 K. MAS frequency and recycle delay were 8.5 kHz and 25 s, respectively.

increasing TOTAPOL concentration, an overall decrease of the signal intensity is observed, which is stronger on the cell wall signals. At 60 mM TOTAPOL, cell wall resonances have almost disappeared from the spectrum, while signals from RNA and lipids are still present. DNP on cells (at least on Gram-positive bacterial cells) at low radical concentration will therefore be very useful for cell wall structural or interaction studies with proteins, antibiotics, or other cells. The study of membrane and cytoplasmic proteins inside of cells might be possible at a higher radical concentration.

Cell wall enhancement and suppression were further confirmed by 2D ^{13}C – ^{13}C correlation experiments at TOTAPOL concentrations of 5 and 60 mM (one-time wash), as shown in Figure 5b,c, respectively. PG and WTA

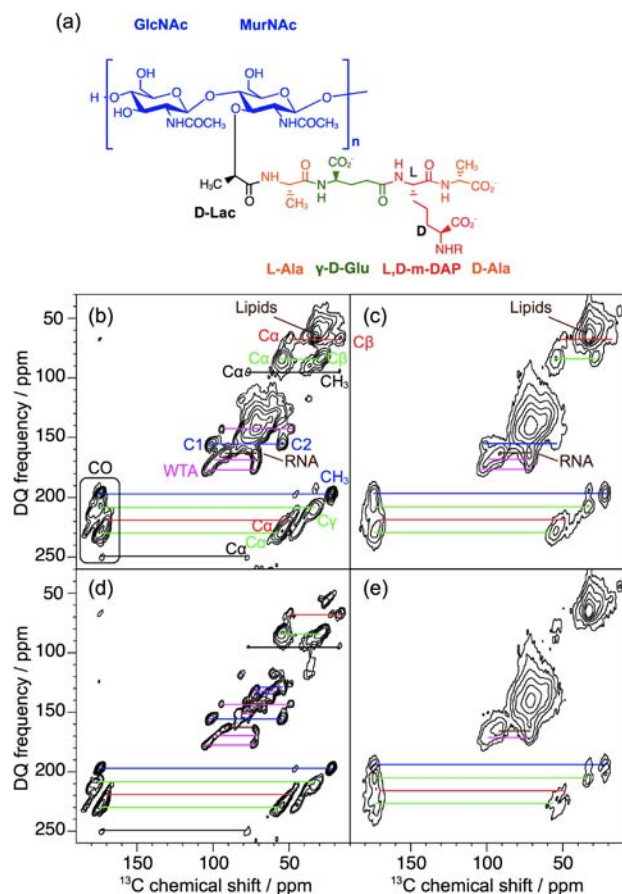


Figure 5. (a) Chemical structure of PG. (b–e) DNP-enhanced 2D double-quantum single-quantum ^{13}C – ^{13}C spectra of EC sample using SPC5 recoupling sequence⁴² at TOTAPOL concentrations of 5 (b) and 60 mM (c). The numbers of scans and the recycle delays were 16 and 4 s for (b) and 256 and 1 s for (c), leading to total experimental times of 4.6 and 14.5 h, respectively. SPC5 mixing time was set to 1.23 ms. Difference spectra are shown in (d) for (b – c) and (e) for (c – b). Respective scaling of combined spectra was adjusted such to end up with positive signals only.

peaks are clearly seen with high signal intensities at 5 mM TOTAPOL concentration (Figure 5b, cell wall enhancement). Those signals are almost suppressed at 60 mM TOTAPOL concentration, while RNA and lipid peaks, already present in the 5 mM spectrum, are still observed (Figure 5c, cell wall suppression). This is illustrated by the PG/RNA and PG/lipids intensity ratios which drop from 0.7 and 0.37, respectively, to 0.37 and 0.045 when going from 5 mM (Figure 5b) to 60 mM TOTAPOL concentration (Figure 5c).

Resolution Improvement of 2D ^{13}C – ^{13}C Correlation Spectra. In an attempt to better separate signals from the different parts of the cell, the 5 mM spectrum (Figure 5b) was subtracted from the 60 mM spectrum (Figure 5c) in such a way that PG signals are completely suppressed (Figure 5e). The large signals of RNA and lipids are still present. This suggests that in the case of an overexpressed membrane protein, its resonances could be observed directly on intact cells without interference from the large cell wall background. Opposite

subtraction (subtracting the 60 mM from the 5 mM spectrum) was carried out as well with relative scaling set such that the lipid signal was suppressed (Figure 5d). Astonishingly, this subtraction leads to an improved spectral resolution, especially visible in the sugar region, where RNA and PG cross-peak patterns can now be partly separated. It seems that the subtraction allows the removal of broad signal components resulting from not only the presence of the radical but also in part from the conformational disorder, as the resolution observed is now even better than the one observed on the reference sample containing no TOTAPOL. This technique proves in our case to be useful in separating resonances of interest from unwanted signals and even improves spectrum resolution that is the major criticism of DNP-enhanced SSNMR.

Considering the strong affinity of TOTAPOL for the cell wall polymers, it may seem curious that the signal intensity of RNA resonances is quite important at low radical concentration (even if their enhancement by DNP is less than for PG) and, respectively, that only weak protein signals are detected. This could be explained by a higher affinity of TOTAPOL for RNA sugars than for proteins, in cases where the polarizing agent can cross the cell wall or the RNA and proteins are released by the lysis of some of the cells.

CONCLUSIONS

We have demonstrated the feasibility of DNP-enhanced SSNMR applied to the study of bacterial cells. TOTAPOL molecules possess a strong binding affinity to PG (or more generally, sugars) and accumulate in the PG layer of the cell wall. This property results from weak noncovalent interactions (probably hydrogen bonding) and does not involve any chemical reaction, keeping thus TOTAPOL molecules active over a long storage period.

The binding affinity can be used to specifically enhance or suppress cell wall signals, for studying either cell wall interactions or other cell components, simply by adjusting radical concentrations. As a result of the nonuniform distribution of radicals in the sample, the property of spectra at low and high concentration of radicals is such that considerable resolution improvement can be obtained by difference spectroscopy. To the best of our knowledge, this type of line-narrowing technique has not yet been reported so far for DNP-enhanced SSNMR. Rationalization of this effect and further investigation are currently on the way in our group in order to enlarge the field of application of this new resolution-enhanced technique for DNP.

Finally, we would also like to emphasize that a real DNP enhancement (ASR) of 24 compared to conventional SSNMR was observed for entire cells, which results in experimental time savings of a factor of 600. With this sensitivity, study at an atomic scale of cell wall interactions for instance can be envisaged that were up to now difficult to detect since only small number of molecules are involved.

It is worth noting that the presented results are not expected to be limited to bacterial cells but could be useful for applications to other type of cells as plant cells or epithelial cells, which both contain sugar units in their cell wall or at their surface. So far, only the biradical TOTAPOL has been investigated for its affinity, which is specific to saccharides. For the selective enhancement of other cell components, the use of other or modified radicals designed for specific interaction with that component can be envisaged, e.g., for

the study of membrane proteins or antimicrobial peptides in interaction with the cell membrane. With the possibility of enhancing specifically cell wall signals and improving resolution, these results pave the way toward a DNP-enhanced on-cell NMR spectroscopy.

■ ASSOCIATED CONTENT

Supporting Information

Discussion on suspension time, details of the experimental conditions, DNP build-up time constants τ_{DNP} for a higher numbers of washing steps (complement to Figure 2), systematic studies of TOTAPOL concentration on EC and DC, discussion on the propagation of DNP-enhanced magnetization, and spectra to explain sample stability. This material is available free of charge via the Internet at <http://pubs.acs.org>.

■ AUTHOR INFORMATION

Corresponding Author

sabine.hediger@cea.fr

Notes

The authors declare no competing financial interest.

■ ACKNOWLEDGMENTS

Dr. Mathilde Giffard and Dr. Lionel Dubois are acknowledged for the synthesis of the TOTAPOL radical. We thank Dr. Bernard Joris and Dr. Ana Amoroso for stimulating discussions. This work was supported by the French National Research Agency through the “programme blanc” (ANR-12-BS08-0016-01) and funding from the RTB.

■ REFERENCES

- (1) Kern, T.; Hediger, S.; Mueller, P.; Giustini, C.; Joris, B.; Bougault, C.; Vollmer, W.; Simorre, J.-P. *J. Am. Chem. Soc.* **2008**, *130*, 5618–5619.
- (2) Sharif, S.; Singh, M.; Kim, S. J.; Schaefer, J. *J. Am. Chem. Soc.* **2009**, *131*, 7023–7030.
- (3) Kern, T.; Giffard, M.; Hediger, S.; Amoroso, A.; Giustini, C.; Bui, N. K.; Joris, B.; Bougault, C.; Vollmer, W.; Simorre, J. P. *J. Am. Chem. Soc.* **2010**, *132*, 10911–10919.
- (4) Dick-Perez, M.; Zhang, Y. A.; Hayes, J.; Salazar, A.; Zabolina, O. A.; Hong, M. *Biochemistry* **2011**, *50*, 989–1000.
- (5) Zhou, X. X.; Cegelski, L. *Biochemistry* **2012**, *51*, 8143–8153.
- (6) Barnes, A. B.; De Paepe, G.; van der Wel, P. C. A.; Hu, K. N.; Joo, C.; Bajaj, V. S.; Mak-Jurkauskas, M. L.; Sirigiri, J. R.; Herzfeld, J.; Temkin, R. J.; Griffin, R. G. *Appl. Magn. Reson.* **2008**, *34*, 237–263.
- (7) Fujiwara, T.; Ramamoorthy, A. In *Annu. Rep. NMR Spectrosc.*; Webb, G. A., Ed.; Elsevier: Amsterdam, The Netherlands, **2006**; Vol. 58, p 155–175.
- (8) Hall, D. A.; Maus, D. C.; Gerfen, G. J.; Inati, S. J.; Becerra, L. R.; Dahlquist, F. W.; Griffin, R. G. *Science* **1997**, *276*, 930–932.
- (9) Rosay, M.; Tometich, L.; Pawsey, S.; Bader, R.; Schauwecker, R.; Blank, M.; Borchard, P. M.; Cauffman, S. R.; Felch, K. L.; Weber, R. T.; Temkin, R. J.; Griffin, R. G.; Maas, W. E. *Phys. Chem. Chem. Phys.* **2010**, *12*, 5850–5860.
- (10) Lee, D.; Takahashi, H.; Thankamony, A. S. L.; Dacquin, J. P.; Bardet, M.; Lafon, O.; De Paepe, G. *J. Am. Chem. Soc.* **2012**, *134*, 18491–18494.
- (11) Lesage, A.; Lelli, M.; Gajan, D.; Caporini, M. A.; Vitzthum, V.; Miéville, P.; Alauzun, J.; Roussey, A.; Thieuleux, C.; Mehdi, A.; Bodenhausen, G.; Copéret, C.; Emsley, L. *J. Am. Chem. Soc.* **2010**, *132*, 15459–15461.
- (12) Renault, M.; Pawsey, S.; Bos, M. P.; Koers, E. J.; Nand, D.; Tommassen-van Bortel, R.; Rosay, M.; Tommassen, J.; Maas, W. E.; Baldus, M. *Angew. Chem., Int. Ed.* **2012**, *51*, 2998–3001.

- (13) Jacso, T.; Franks, W. T.; Rose, H.; Fink, U.; Broecker, J.; Keller, S.; Oschkinat, H.; Reif, B. *Angew. Chem., Int. Ed.* **2012**, *51*, 432–435.
- (14) Vollmer, W.; Blanot, D.; de Pedro, M. A. *FEMS Microbiol. Rev.* **2008**, *32*, 149–167.
- (15) Chaput, C.; Boneca, I. G. *Microbes Infect.* **2007**, *9*, 637–647.
- (16) Lebeer, S.; Vanderleyden, J.; De Keersmaecker, S. C. *J. Nat. Rev. Microbiol.* **2010**, *8*, 171–184.
- (17) Song, C.; Hu, K. N.; Joo, C. G.; Swager, T. M.; Griffin, R. G. *J. Am. Chem. Soc.* **2006**, *128*, 11385–11390.
- (18) van der Wel, P. C. A.; Hu, K. N.; Lewandoski, J.; Griffin, R. G. *J. Am. Chem. Soc.* **2006**, *128*, 10840–10846.
- (19) Bajaj, V. S.; Mak-Jurkauskas, M. L.; Belenky, M.; Herzfeld, J.; Griffin, R. G. *Proc. Natl. Acad. Sci. U.S.A.* **2009**, *106*, 9244–9249.
- (20) Reggie, L.; Lopez, J. J.; Collinson, I.; Glaubitz, C.; Lorch, M. *J. Am. Chem. Soc.* **2011**, *133*, 19084–19086.
- (21) Lange, S.; Linden, A. H.; Akbey, U.; Franks, W. T.; Loening, N. M.; van Rossum, B. J.; Oschkinat, H. *J. Magn. Reson.* **2012**, *216*, 209–212.
- (22) Rossini, A. J.; Zagdoun, A.; Lelli, M.; Gajan, D.; Rascon, F.; Rosay, M.; Maas, W. E.; Copéret, C.; Lesage, A.; Emsley, L. *Chem. Sci.* **2012**, *3*, 108–115.
- (23) Takahashi, H.; Lee, D.; Dubois, L.; Bardet, M.; Hediger, S.; De Paepe, G. *Angew. Chem., Int. Ed.* **2012**, *51*, 11766–11769.
- (24) Linden, A. H.; Franks, W. T.; Akbey, U.; Lange, S.; van Rossum, B. J.; Oschkinat, H. *J. Biomol. NMR* **2011**, *51*, 283–292.
- (25) Siemer, A. B.; Huang, K. Y.; McDermott, A. E. *Plos One* **2012**, *7*, e47242.
- (26) Rossini, A. J.; Zagdoun, A.; Hegner, F.; Schwarzwald, M.; Gajan, D.; Coperet, C.; Lesage, A.; Emsley, L. *J. Am. Chem. Soc.* **2012**, *134*, 16899–16908.
- (27) Renault, M.; Tommassen-van Bortel, R.; Bos, M. P.; Post, J. A.; Tommassen, J.; Baldus, M. *Proc. Natl. Acad. Sci. U.S.A.* **2012**, *109*, 4863–4868.
- (28) Harris, C. L.; Toner, M.; Hubel, A.; Cravalho, E. G.; Yarmush, M. L.; Tompkins, R. G. *Cryobiology* **1991**, *28*, 436–444.
- (29) Loretz, L. J.; Li, A. P.; Flye, M. W.; Wilson, A. G. E. *Xenobiotica* **1989**, *19*, 489–498.
- (30) Severin, A.; Tomasz, A. *J. Bacteriol.* **1996**, *178*, 168–174.
- (31) Girardin, S. E.; Boneca, I. G.; Carneiro, L. A. M.; Antignac, A.; Jehanno, M.; Viala, J.; Tedin, K.; Taha, M. K.; Labigne, A.; Zahringer, U.; Coyle, A. J.; Bertin, J.; Sansonetti, P. J.; Philpott, D. J. *Science* **2003**, *300*, 1584–1587.
- (32) Kessenikh, A. V.; Manenkov, A. A.; Pyatnitskii, G. I. *Sov. Phys. Solid State* **1964**, *6*, 641–643.
- (33) Hwang, C. F.; Hill, D. A. *Phys. Rev. Lett.* **1967**, *19*, 1011–1013.
- (34) Wollan, D. S. *Phys. Rev. B* **1976**, *13*, 3671–3685.
- (35) Maly, T.; Debelouchina, G. T.; Bajaj, V. S.; Hu, K. N.; Joo, C. G.; Mak-Jurkauskas, M. L.; Sirigiri, J. R.; van der Wel, P. C.; Herzfeld, J.; Temkin, R. J.; Griffin, R. G. *J. Chem. Phys.* **2008**, *128*, 052211.
- (36) Hu, K. N.; Song, C.; Yu, H. H.; Swager, T. M.; Griffin, R. G. *J. Chem. Phys.* **2008**, *128*, 052302.
- (37) Hu, K. N.; Debelouchina, G. T.; Smith, A. A.; Griffin, R. G. *J. Chem. Phys.* **2011**, *134*, 125105.
- (38) Negoro, M.; Nakayama, K.; Tateishi, K.; Kagawa, A.; Takeda, K.; Kitagawa, M. *J. Chem. Phys.* **2010**, *133*, 154504.
- (39) Takahashi, H.; Akutsu, H.; Fujiwara, T. *J. Chem. Phys.* **2008**, *129*, 154504.
- (40) Linden, A. H.; Lange, S.; Franks, W. T.; Akbey, U.; Specker, E.; van Rossum, B. J.; Oschkinat, H. *J. Am. Chem. Soc.* **2011**, *133*, 19266–19269.
- (41) Akbey, U.; Franks, W. T.; Linden, A.; Lange, S.; Griffin, R. G.; van Rossum, B. J.; Oschkinat, H. *Angew. Chem., Int. Ed.* **2010**, *49*, 7803–7806.
- (42) Hohwy, M.; Rienstra, C. M.; Jaroniec, C. P.; Griffin, R. G. *J. Chem. Phys.* **1999**, *110*, 7983–7992.